Minerals Engineering 179 (2022) 107446

Contents lists available at ScienceDirect

Minerals Engineering

journal homepage: www.elsevier.com/locate/mineng

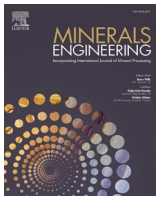

Enhanced acid leaching of rare earths from NdCeFeB magnets

Iryna Makarava [a,*], Aliaksandr Kasach [b], Dzmitry Kharytonau [c], Irina Kurilo [d], Markku Laatikainen [a], Eveliina Repo [a]

[a] Department of Separation Science, School of Engineering Science, LUT University, Yliopistonkatu 34, FI-53850, Finland
[b] Department of Chemistry, Technology of Electrochemical Production and Electronic Engineering Materials, Belarussian State Technological University, Sverdlova 13a, 220050 Minsk, Belarus
[c] Jerzy Haber Institute of Catalysis and Surface Chemistry, Polish Academy of Sciences, Niezapominajek 8, 30-239 Krakow, Poland
[d] Department of Physical, Colloid, and Analytical Chemistry, Belarussian State Technological University, Sverdlova 13a, 220050 Minsk, Belarus

ARTICLE INFO

Keywords:
Electrolysis
Leaching
Rare-earth elements
NdCeFeB magnet
Oxalic acid

ABSTRACT

Development of the effective technology for recovery of critical rare-earth elements (REEs) from end-of-life permanent magnets is one of the important technological challenges. In this study, chemical and electrochemical leaching of NdCeFeB magnets was investigated in 0.5 mol/L sulfuric acid containing varying concentration of oxalic acid. The influence of $H_2C_2O_4$ concentration on leaching efficiency and morphological properties of the NdCeFeB surface, as well as on the chemical composition and ζ-potential of the oxalate precipitate particles was discussed. Efficient separation of REEs can be achieved at $H_2C_2O_4$ concentrations of 0.05–0.20 mol/L and the maximum REE purity was 97.2%. In electrochemical leaching, the leaching rate was substantially higher than in chemical leaching, where blocking of the magnet surface by precipitate layer was observed.

1. Introduction

The growth of population and development of advanced technologies have led to higher and higher consumption of specific elements, so called critical materials, which are in high supply risk and of economic importance (El Wali et al., 2021; Golroudbary et al., 2020, 2019). Many studies have mentioned rare-earth elements (REEs) as critical materials due to geochemical (Costis et al., 2021) and political (Ciacci et al., 2019) challenges with mining, and to their necessity for a wide range of applications. The amount of globally mined REEs in 2020 was around 240 000 t (Ore et al., 2021). Around 23% of the primary REEs are used to produce neodymium magnets (NdFeB). So-called NdFeB permanent magnets consist of iron (50–70%), boron (1%), and 25–30% of REEs (mainly neodymium) (Turpeinen et al., 2019) (Berzi et al., 2019). Nowadays, for many magnetic applications, a large part of Nd (from 10 to 15%) is substituted by Ce, which is the least favorable REE for hard magnetic applications, but is widely used because of higher crustal abundance and low-cost (Arsad and Ibrahim, 2016; Li et al., 2015; Ni et al., 2016; Xu et al., 2016; Yang et al., 2017a). Permanent magnets are currently the strongest magnetic materials and found applications in audio systems, automotive (conventional and electric vehicles), refrigerators, air conditioners, wind turbines, magnetic resonance imaging (MRI) machines, etc. (Binnemans and Jones, 2014; Peeters et al., 2018; Schreiber et al., 2019). In this line, conventional and electric vehicles together with wind turbines consume more than 50% of all magnets, hence, their end-of-life products can be considered as a valuable product for recycling. Currently, around 12 million of electric vehicles –1 to 5 kg of permanent magnets in each – and around 1 million of wind turbines – each containing 1–2 t of permanent magnets – are in service globally (Reimer et al., 2020), with the life time ranging 12–15 and 20–30 years, respectively (Yang et al., 2017b). Even if we consider that only 25% of large motor and wind turbines could be collected for recycling, ca. 140 000 t of magnets for secondary source would be available in near future. For this reason, an effective technology for recycling of spent neodymium magnets will allow to bring back useful materials, solve the problem of Nd demand, and decrease negative ecological impact of these waste.

Hydrometallurgical technologies for recycling of neodymium magnets are more promising than pyrometallurgical ones due to lower energy consumption (Liu et al., 2020; Önal et al., 2020; Tian et al., 2019). The main hydrometallurgical step is the conversion of solid material into a liquid state (leaching). Different mineral (Kumari et al., 2018; Peelman

* Corresponding author.
E-mail address: Iryna.Makarava@lut.fi (I. Makarava).

https://doi.org/10.1016/j.mineng.2022.107446
Received 17 November 2021; Received in revised form 1 February 2022; Accepted 6 February 2022
Available online 13 February 2022

Table 1
Chemical composition of spent NdCeFeB magnets based on ICP-MS data.

Element, wt%							
Fe	Co	Cu	Ce	Pr	Nd	Gd	Others
68.25	0.01	0.19	13.58	1.99	8.51	7.39	Balance

et al., 2015; Yang et al., 2020) and organic acids (Reisdörfer et al., 2019) were used for leaching of neodymium magnets. Further treatment includes precipitation of REEs in the form of oxalates, hydroxides, or double salts. It is well-known that oxalic acid $H_2C_2O_4$ is an efficient precipitant of REEs (oxalates of REEs have $pK_{sp} = 31–33$) (Marins et al., 2020; Zhang et al., 2020). Oxalic acid can be directly used during electrochemical dissolution (Makarova et al., 2020a; Makarova et al., 2020b) or after leaching step to precipitate a mixture of REEs (Jorjani and Shahbazi, 2016; Lai et al., 2014; Önal et al., 2020; Venkatesan et al., 2018). It was reported (Makarova et al., 2020b) that the addition of oxalic acid $H_2C_2O_4$ to the sulfuric acid solution decreases voltage on the bath and increases buffer capacity of the electrolyte. This allowed to decrease economic losses and increase operational life of the electrolyte. Liu et al. (Liu et al., 2021), proposed to recover REEs and iron from neodymium magnets via chemical leaching only in oxalic acid. Before leaching, however, mechanical pre-treatment and roasting at 900 °C were used, leading to high energy consumptions.

To the best of our knowledge, there are only a few studies on electrochemical treatment of neodymium magnets (Abbasalizadeh et al., 2019; Venkatesan et al., 2018). Electrochemical methods have the following advantages compared to thermal treatment and chemical dissolution. (1) to eliminate the milling stage by conducting the process of dissolution of REEs directly from bulk waste; (2) to intensify the process of leaching (Makarova et al., 2020b); (3) to selectively extract REEs directly during anodic leaching of waste (Makarova et al., 2020a); (4) to exclude additional cost of reagents in comparison with the chemical oxidation of the components of the magnets; (5) to prevent the formation of hazardous harmful by-products; (6) to reuse working solutions; (7) to automate the processing of leaching.

This work is a continuation of our previous studies on chemical and electrochemical leaching from oxalate-based solutions (Makarova et al., 2020a, 2020b), where concentration of oxalate ions in the solution was kept constant at 0.05 mol/L. The key finding of our previous study (Makarova et al., 2020a) states that in a mixture of 0.5 mol/L H_2SO_4 and 0.05 mol/L $H_2C_2O_4$ during electro-leaching of the spent NdFeB magnet at current density of 50 A/dm^2, the even and homogenous deposition of the REEs on the cathode and anodic dissolution of NdCeFeB can be achieved. However, it is worth mentioning that the proposed technology suffers from a low efficiency of REEs recovery, and either mechanical or chemical removal of oxalate precipitate from the cathodic substrate for further purification is required. Moreover, we have shown (Makarova et al., 2020b) that it is possible to obtain REEs oxalate not on the surface of the cathode but in the volume of the electrolyte, which, in turn, underlines the necessity of examining the influence of oxalic acid concentration on the oxalate precipitation during the electro-leaching.

The aim of this work is to understand the influence of $H_2C_2O_4$ concentration on physico-chemical properties of rare-earth oxalates formed during leaching of cerium-neodymium magnets (NdCeFeB) in sulfuric acid solutions. Number of analytical and physico-chemical methods (SEM, EDX, XRD, ζ-potential) were used to investigate the composition, structure, and surface charge of the oxalate precipitate.

2. Experimental

2.1. Materials

Spent NdCeFeB magnets from REDMAG JSC (Russia) with a diameter of 30 mm and a thickness of 5 mm were used in all experiments.

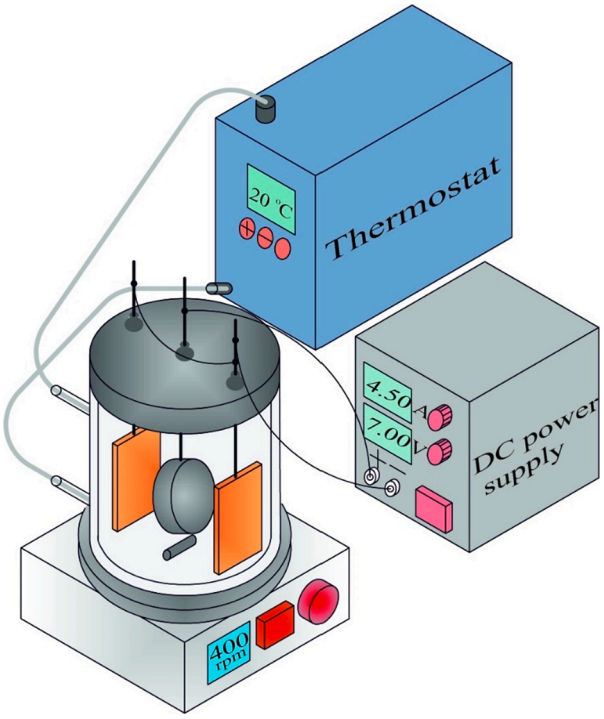

Fig. 1. Schematic illustration of the setup for electro-leaching of NdCeFeB magnets.

Demagnetization and mechanical/chemical pre-treatment of the magnets are described in detail in our previous study (Makarova et al., 2020b). The chemical composition determined by inductively coupled plasma mass spectrometry (ICP-MS) is reported in Table 1.

Mixtures of sulfuric (Sigma-Aldrich, 98%) and oxalic acid (Sigma-Aldrich, >97.5%) were used as the leaching agent. Solutions were prepared by diluting acids with MilliQ water of 18.2 MΩ cm resistivity (Merck Millipore Q-POD).

2.2. Electrochemical leaching

The setup for electrochemical leaching of NdCeFeB magnets is presented in Fig. 1.

In leaching experiments, an NdCeFeB magnet was used as the anode and two copper plates (surface area 3 cm × 5 cm) were used as the cathodes as shown in Fig. 1. The concentration of sulfuric acid was kept constant at 0.5 mol/L and the concentration of oxalic acid was 0, 0.01, 0.05, 0.10, or 0.20 mol/L. The solid-to-liquid ratio was kept at 0.06 dm^2 of the NdCeFeB surface per 150 mL of the solution, and the stirring rate was 400 rpm. The maximum duration of electro-leaching was 1 h. After electrolysis, electrodes and obtained precipitates were thoroughly washed, air-dried, and weighted. The precipitates were dried for 4 h at 80 °C before weighting. Detailed description of leaching experiments can be found in (Makarova et al., 2020a).

2.3. Electrochemical measurements

Electrochemical measurements of the dissolution process of NdCeFeB magnets were carried out in a three-electrode cell with the side location of the working electrode using a potentiostat–galvanostat (PGSTAT 302 N, Methrom Autolab). A saturated silver/silver chloride electrode was used as the reference electrode, a platinum grid as the counter electrode, and the NdCeFeB magnet with the exposed surface area of 1 cm^2 as the working electrode. Prior to experiments, working electrodes were immersed in the electrolyte for 30 min. Linear polarization scans were carried out at a sweep rate of 5 mV/s in the range of

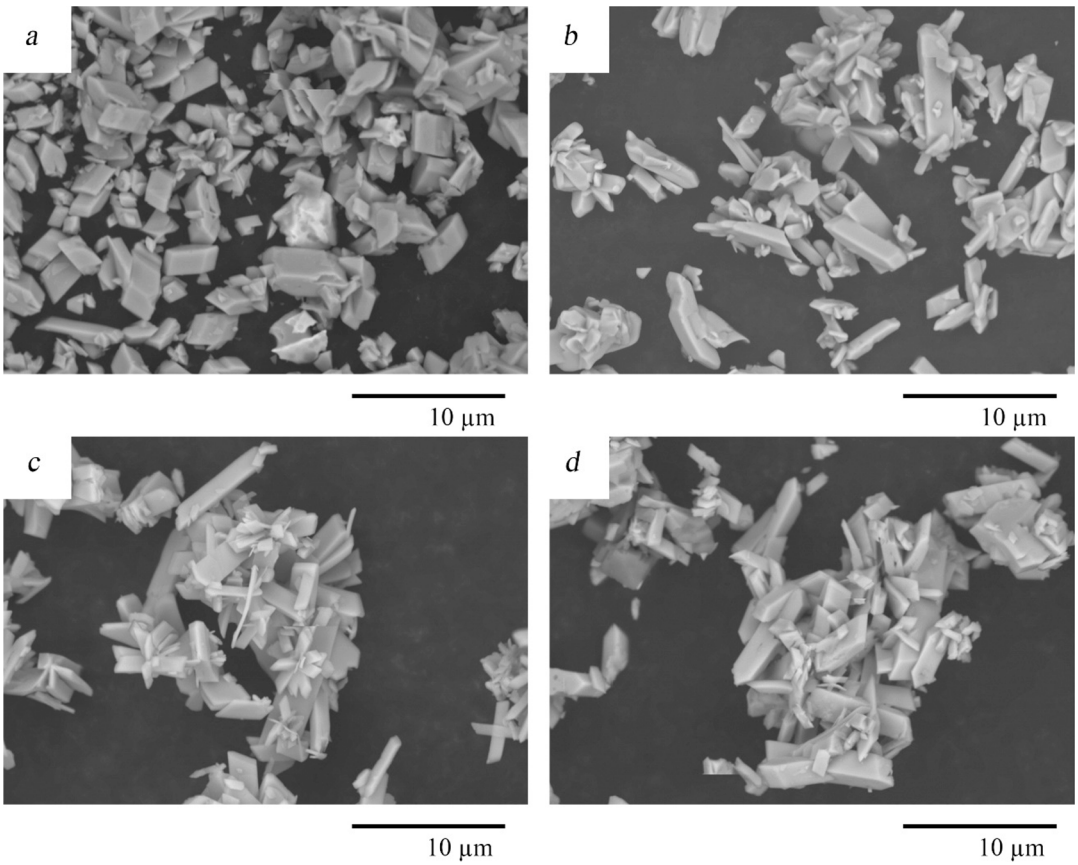

Fig. 2. SEM images of REE oxalate crystals obtained in 0.5 mol/L H_2SO_4 solution with different concentration of $H_2C_2O_4$: (*a*) 0.01 mol/L; (*b*) 0.05 mol/L; (*c*) 0.1 mol/L, (*d*) 0.2 mol/L.

potentials from –300 mV to +300 mV from the open circuit potential (OCP). By linear fitting of Tafel $E - \log i$ curves (Makarova et al., 2019), dissolution current densities i_{diss} were obtained. Temperature of 22 ± 1 °C was controlled by a water jacket and a thermostat.

2.4. Characterization methods

The surface morphology and composition of the NdCeFeB anode and the oxalate precipitate were examined using a Hitachi SU3500 scanning electron microscope (SEM) equipped with an energy dispersive X-ray (EDX) unit. The chemical composition and crystal structure of the oxalate precipitates after electrolysis were further ascertained using X-ray diffraction (XRD) (a Bruker D8 Advance) with Cu K_α irradiation. The 2θ range was 10–50° and a step size was 0.02°/s.

Oxalate precipitates, which were obtained during electro-leaching in the mixtures of sulfuric and oxalic acids, were filtered every 15 min and washed thoroughly with water, dried for 4 h at 80 °C, and digested. The filtered digestion solution was analyzed with inductively coupled plasma mass spectroscopy (an ICP-MS, Agilent 7900) in a mixture of 1% HNO_3 and 1% HCl (Ultrapure, Merck). Relative standard deviation of all ICP measurements were less than 3.6%.

ζ-potential of neodymium oxalate particles was measured by a Zetasizer ZS Nano (Malvern) analyzer. The precipitate was thoroughly washed, filtered, and dried. The pH in the analyzed solution was adjusted to 1.0 with 1 mol/L HCl solution. Electrophoretic light scattering method was utilized for the ζ-potential measurement according to methodology developed by Malvern Instruments using the surface zeta potential cell (zen1020, Malvern Instruments) and the zeta potential transfer standard (DTS1235, Malvern Instruments) as tracer particle (zeta potential −42.0 mV ± 4.2 mV). The Smoluchowski model was used to calculate ζ-potential values of nanoparticles in aqueous media (Lu et al., 2018).

2.5. Efficiency of electro-leaching

For assessment of the electrodeposition conditions, current efficiencies of anodic (ε_a) and cathodic (ε_c) processes were calculated. For iron, electrochemical equivalent is $q_{Fe} = M_{Fe}/z_{Fe}F = 1.05$ g/(Ah), for neodymium $q_{Nd} = 1.79$ g/(Ah), for cerium $q_{Ce} = 1.74$ g/(Ah), and for praseodymium $q_{Pr} = 1.75$ g/(Ah), where z is the ion charge and F is the Faraday constant. $q_{alloy} = 1.196$ g/(Ah) was obtained using the composition given in Table 1.

$$q_{alloy} = \frac{1}{\frac{w_{Fe}}{q_{Fe}} + \frac{w_{Nd}}{q_{Nd}} + \frac{w_{Ce}}{q_{Ce}} + \frac{w_{Pr}}{q_{Pr}}}, \quad (1)$$

$$\varepsilon_a = \frac{\Delta m_a}{i S_a q_{alloy} \tau}, \quad (2)$$

$$\varepsilon_c = \frac{\Delta m_c}{i S_c q_{Fe} \tau}, \quad (3)$$

where w_{Fe}, w_{Nd}, w_{Ce}, and w_{Pr} are weight fractions of iron, neodymium, cerium, and praseodymium in the magnet, respectively; i is current density, A/dm^2; S is the surface area of electrode (S_a and S_c of anode and cathode, respectively); Δm_a and Δm_c are weight of dissolved NdCeFeB magnet and cathodic sediment, g, respectively; τ is time of leaching, h.

Selectivity of process were considered according to two parameters: the purity of the REE oxalate precipitate, P, and REE precipitate yield, Y, which were calculated from Eqs. (4) and (5).

$$P = \frac{m_{REE}^{dep}}{m_{REE}^{dep} + m_{others}^{dep}} \cdot 100\% \quad (4)$$

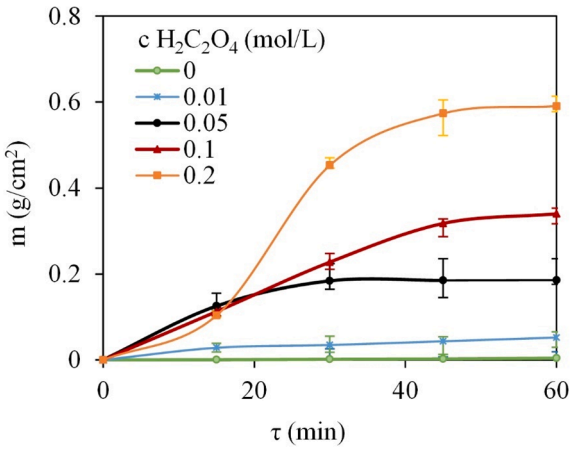

Fig. 3. Precipitation of REE oxalates during electro-leaching of NdCeFeB magnet in 0.5 mol/L H_2SO_4 solutions with different concentrations of oxalic acid, $i_a = 50$ A/dm^2.

$$Y = \frac{m_{REE}^{dep}}{m_{REE}^{dep} + m_{REE}^{sol}} \cdot 100\% \quad (5)$$

where m_{REE}^{dep} and m_{others}^{dep} are weights of REEs and other metals in the precipitate, m_{REE}^{sol} is weight of REEs in the solution.

All experiments were done in triplicate to ensure statistical reliability of the results.

3. Results and discussion

3.1. Characterization of precipitates formed in solutions

When the NdCeFeB magnet was electro-leached in the presence of oxalic acid, REE oxalates precipitated as elongated crystals with an average size around 1–2 μm (Fig. 2). Color of crystals varied from light pink to yellow.

Amount of the precipitate formed during electro-leaching strongly depends on the initial $H_2C_2O_4$ concentration as depicted in Fig. 3. Here, the y-axis gives the weight of the metal oxalate per unit area of the magnet surface. In the presence of 0.01 mol/L $H_2C_2O_4$, 0.028 g/cm^2 of the precipitate was formed after 15 min and further increase in the duration of electro-leaching only slightly increased the amount of the formed precipitate. An increase in the initial concentration of $H_2C_2O_4$ lead to a significant weight gain of the formed precipitate. The values at 60 min depend nearly linearly on the oxalate concentration suggesting that the amount of oxalate is the limiting factor.

According to the mass balances in the case of 0.05 mol/L $H_2C_2O_4$, oxalic acid should be fully consumed at around 90 min. Nevertheless, according to the experimental data (Fig. 3), a constant weight of the precipitate was achieved already after 45 min. It indicates that part of the oxalate ions is consumed by formation of soluble complexes with iron.

The metal distribution in the precipitate at different time of leaching and concentration of $H_2C_2O_4$ in the electrolyte is presented in Fig. 4.

According to Fig. 4a and b, almost constant REE distribution was found in the precipitate and it is identical with the distribution in the magnet. The only exception is Ce, which appear to follow an opposite trend with iron; in Fig. 4a the iron content increases with time and Ce

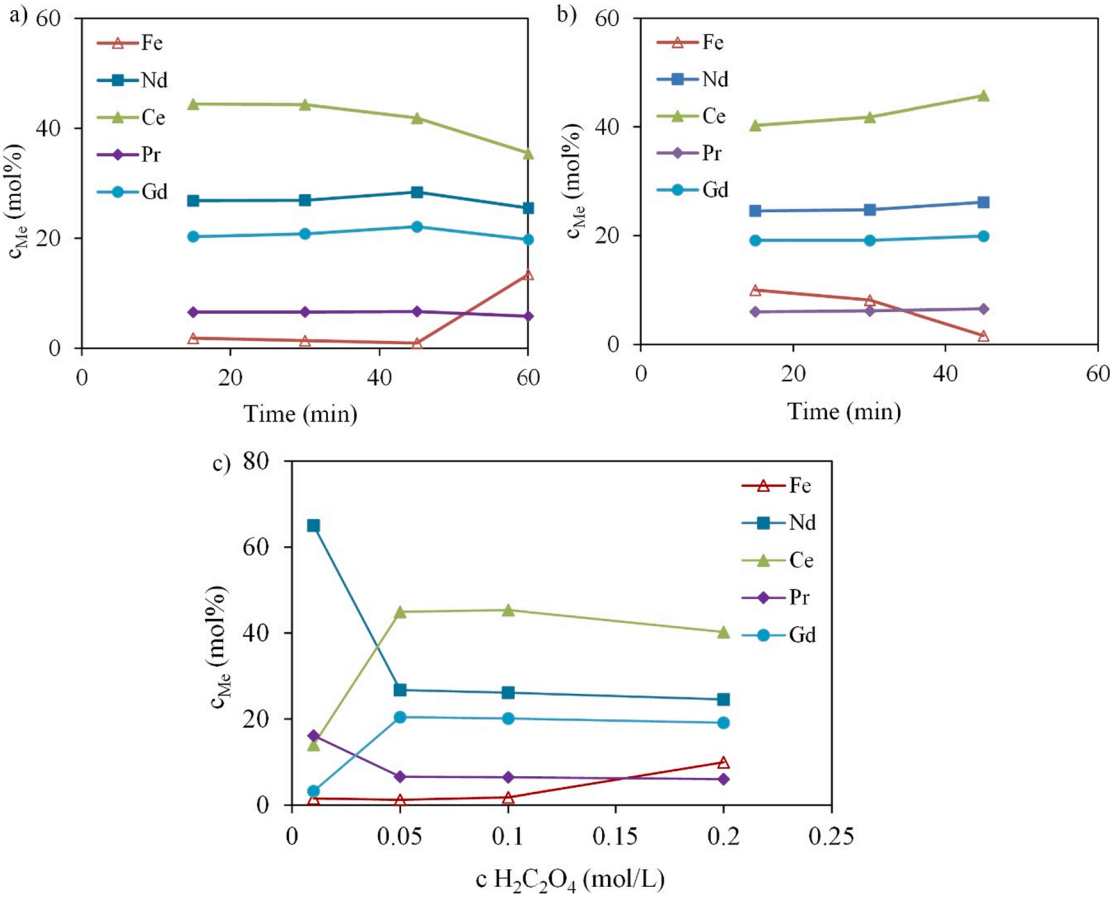

Fig. 4. Concentration of metal ions in the oxalate precipitate depending on leaching time in 0.5 mol/L H_2SO_4 containing (*a*) 0.1 mol/L $H_2C_2O_4$ and (*b*) 0.2 mol/L $H_2C_2O_4$; (*c*) concentration of oxalic acid (after 15 min of electrolysis).

Table 2
REE purity (P, %) and precipitation yield (Y, %) in leaching of NdCeFeB magnets by 0.5 mol/L sulfuric acid containing different concentrations of oxalic acid.

Time, min	Electrochemical leaching								Chemical leaching
	Concentration of $H_2C_2O_4$, M								
	0.01		0.05		0.10		0.20		0.05
	P, %	Y, %	P, %	Y, %	P, %	Y, %	P, %	Y, %	P, %
15	96.7	30.5	97.2	96.4	96.7	99.7	94.2	96.1	–
30	–	–	95.7	97.2	97.2	95.6	94.1	93.4	96.8
45	–	–	–	–	86.4	95.2	97.2	97.3	90.5
60	–	–	–	–	85.4	–	–		86.8

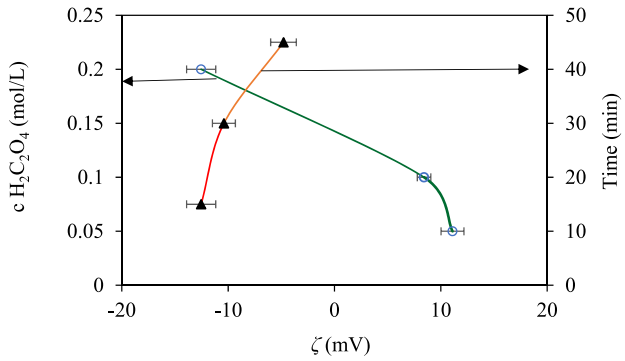

Fig. 5. Dependence of zeta potential of the oxalate precipitate on the concentration of oxalic acid at $t = 15$ min and on leaching time at $c_{H_2C_2O_4} = 0.2$ M.

content decreases, while in Fig. 4b the opposite was true. At very low oxalate concentrations, some REE selectivity was observed. In the solution containing 0.01 mol/L $H_2C_2O_4$, neodymium and praseodymium oxalates were preferentially precipitated. The concentration of $Nd_2(C_2O_4)_3$ decreased approximately 2 times by increasing the concentration of oxalic acid and starting from the concentration of 0.05 M, $Ce(C_2O_4)_3$ became the major component of the precipitate. The same trend was observed by Ni et al. (Ni et al., 2016) and it is probably due to the distribution of the metals in the magnet structure. Nd and Pr are located in the REE-rich phase, while Ce is concentrated in the Fe-rich phase. Increasing time of electrolysis (Fig. 4a) and the concentration of oxalic acid (Fig. 4c) leads to decreasing of the purity of the oxalate precipitate (Table 2) as the amount of iron in the precipitate increases up to 10 mol%.

The REE purity of the oxalate precipitate varied from 85 to 97 %. Increasing of electrolysis time from 15 to 60 min decreases the purity of the precipitate by 5–10% under all examined conditions because the solution accumulates iron ions. Yield of the REE oxalate precipitate is more than 95% for solutions with concentration of $H_2C_2O_4$ from 0.05 to

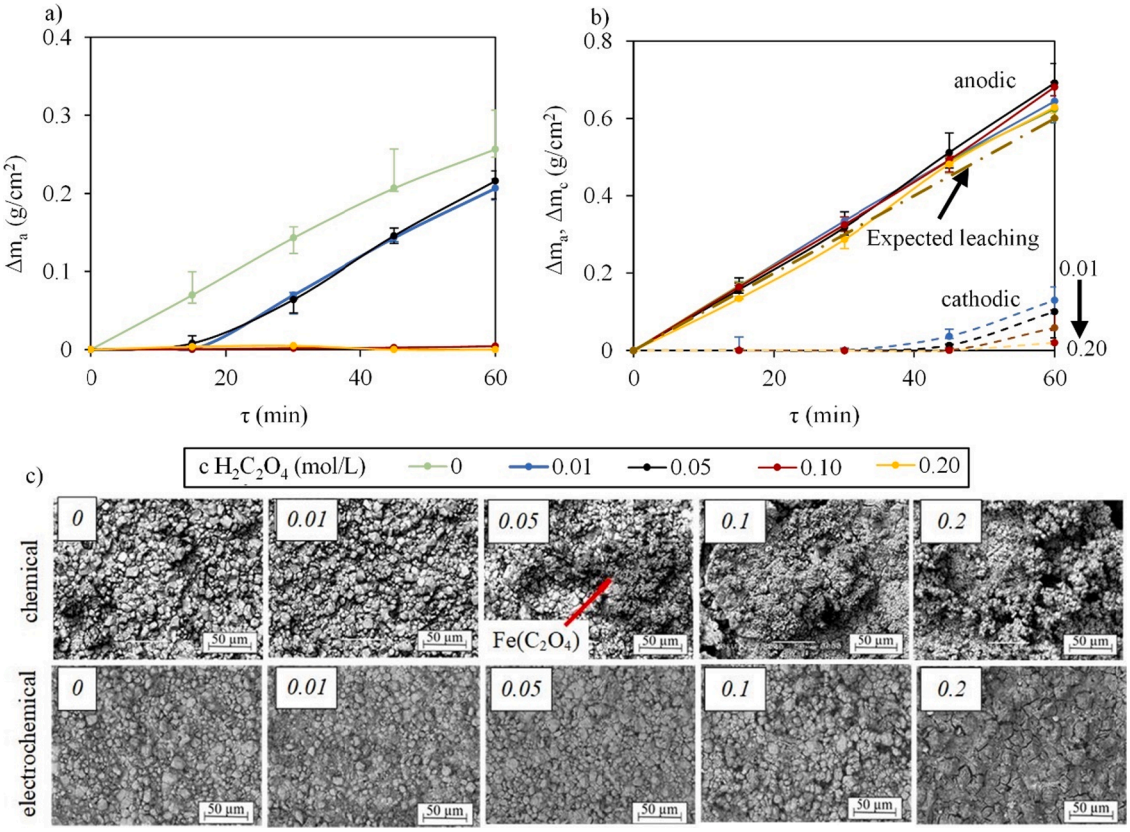

Fig. 6. Weight loss of NdCeFeB magnets during chemical leaching (*a*) and electro-leaching (*b*) in 0.5 mol/L H_2SO_4 with different concentrations of oxalic acid. Dashed lines correspond to weight increase on cathode due to iron reduction and the numbers indicate oxalate concentration. $i_a = 50$ A/dm^2. Surface scans (*c*) were taken after 60 min of leaching. Expected electrochemical leaching corresponds to theoretical leaching value calculated by the Faraday's law.

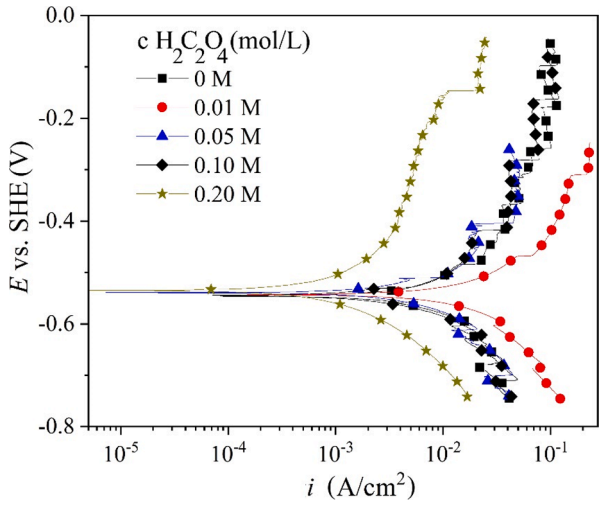

Fig. 7. Linear potentiodynamic polarization curves of NdCeFeB magnets in 0.5 mol/L H_2SO_4 and different concentration of oxalic acid (0–0.2 M).

0.2 mol/L and 30.5% for 0.01 mol/L of $H_2C_2O_4$.

The purity of the oxalate precipitate is linked with the surface charge of the precipitate, as a part of it could be lost by inclusion to cathodic iron deposit (Makarova et al., 2020a). Zeta-potential of the oxalate precipitate depends on leaching time and on the concentration of oxalic acid as depicted in Fig. 5.

Zeta potential of the REE-oxalate precipitate became more positive at low concentrations of oxalic acid, which can lead to specific adsorption of the oxalate precipitate on the cathode (0.05 mol/L $H_2C_2O_4$, $\zeta = 11.1$ mV) (Makarova et al., 2020a, 2020b). Increasing of time of electrolysis from 15 to 45 min leads to increasing of negative charge on REE oxalate from −12.5 to −4.8 mV.

3.2. *Influence of oxalic acid on anodic and cathodic processes during NdCeFeB leaching*

The process of recovery of REEs from NdCeFeB magnets in the form of oxalates cannot be fully explained without examination of the anodic dissolution and the processes of the cathodic reduction.

Anodic dissolution of NdCeFeB magnets gives Nd^{3+}, Ce^{3+}, Pr^{3+} and Fe^{2+} ions as primary soluble species. In the presence of oxalic acid, REE ions form insoluble oxalates $REE_2(C_2O_4)_3{\cdot}10H_2O(s)$, while iron ions form soluble complexes $[Fe(C_2O_4)_n]^{2-2n}(aq)$ and possibly also insoluble compounds (Pliego et al., 2014; Salmimies et al., 2016). Some solubilization of REEs may occur via mixed oxalates of the type $REEFe(C_2O_4)_3$ (Lin et al., 2012). Thus, the addition of $H_2C_2O_4$ into the leaching solution leads to the formation of poorly soluble oxalates, which can partially block the electrode surface, thereby increasing the anodic polarization.

The weight loss of NdCeFeB magnets during chemical leaching (*a*) and electro-leaching (*b*) in 0.5 mol/L H_2SO_4 solutions with varying concentration of $H_2C_2O_4$ is shown in Fig. 6. The SEM scans in Fig. 6c indicate surface morphology after 60 min of leaching.

The dissolution rate in chemical (Fig. 6a) and electrochemical (Fig. 6b) leaching was 0.26 g/(cm^2h) and 0.59–0.63 g/(cm^2h), respectively. It shows that the electrochemical leaching has 2.0–2.5 times higher dissolution rate of NdCeFeB as compared with the chemical one. The anode current efficiency of electro-leaching exceeded 100% and varied from 104 to 108%, which could be explained by the contribution of chemical leaching. Increase in the $H_2C_2O_4$ concentration during chemical leaching to 0.05 mol/L lead to a decrease in the dissolution rate to 0.22 g/(cm^2h). The kinetics of leaching of individual elements (iron and REEs) is presented in Fig. 2S and 3S in the supplementary material. In the concentration range of 0.1–0.2 mol/L $H_2C_2O_4$, the leaching process was completely suppressed. Under these conditions, a significant fraction of the magnet surface became covered with an insoluble layer with the following composition: C – 27.06 mol-%, O – 60.74 mol-%, Fe – 9.33 mol-%, Ce – 1.62 mol-%, Nd – 0.62 mol-%, Gd – 0.63 mol-%. These values roughly correspond to the structure of ferrous oxalate, $Fe(C_2O_4)$, with some inclusion of $REE_2(C_2O_4)_3$. In contrast to chemical leaching (22 ± 1 °C), variation of the oxalic acid concentration in the range of 0–0.2 mol/L did not significantly affect the dissolution rate during electro-leaching. The anodic treatment thus promotes detachment of the passive layer of insoluble oxalates from the magnet surface due to intensive oxygen evolution.

Table 3
Cathodic current efficiency and dissolution current density of NdCeFeB depending on concentration of oxalic acid and time of electro-leaching.

Time, min	Cathodic current efficiency, %				
	0	0.01	0.05	0.1	0.2
30–45	18.0	17.0	9.0	0.4	0.2
45–60	73.5	62.7	58.6	39.0	13.4
	Dissolution current density of NdCeFeB, 10^{-4} A/cm^2				
	7.60 ± 1.10	8.39 ± 0.89	7.11 ± 1.22	6.79 ± 0.83	3.53 ± 0.4

Although there was no evidence of passivation of the magnet surface during electro-leaching, the EDX analysis showed areas rich in oxygen. The content of oxygen on the surface of the NdCeFeB magnet increases from 4.6 to 30.1 wt-%, when the concentration of $H_2C_2O_4$ increase from 0 to 0.2 mol/L (Table S1, Supplementary material). The possibility of the passivation was also suggested by OCP measurements and by chronopotentiograms obtained at the anodic current density of 50 A/dm^2 (Fig. 1S, supplementary material). Similar behavior was found by linear potentiodynamic polarization curves of the NdCeFeB magnet in the mixtures of sulfuric and oxalic acids (Fig. 7). The dissolution current densities were estimated by linear fitting from the polarization curves represented in Fig. 7. As shown in Table 3, increasing the $H_2C_2O_4$ concentration from 0.01 to 0.2 mol/L led to almost four-fold decrease in the dissolution current density.

Deposition of iron on the cathode during the electrochemical leaching in 0.5 mol/L H_2SO_4 with varying content of $H_2C_2O_4$ is illustrated in Fig. 6. During the first 30 min, only hydrogen evolution occurs, while a slight weight gain after 30 min is observed at the cathode mainly due to the reduction of Fe^{2+} ions. Increasing of time of electrolysis leads to a gradual growth of the electrodeposition rate of Fe^{2+} ions. Increasing of the $H_2C_2O_4$ concentration leads to a decrease of the mass of the cathode deposit. The Faradic current efficiency (CE) of the reduction process is shown in Table 3. A lower amount of the consumed current for the cathodic reduction of iron at lower concentrations of $H_2C_2O_4$ may be the result of the following factors.

(1) Sufficiently stable complex compounds $[Fe(C_2O_4)_n]^{2-2n}$ and $[Fe(C_2O_4)_n]^{3-3n}$ are formed in the solution, the discharge of which occurs at more negative potentials than in the case of the reduction of uncomplexed iron(II) and iron(III) ions. Thus, the binding of iron ions into complex compounds increases the fraction of the current that is spent on the reduction of hydrogen ions.
(2) pH of the electrolyte has a direct effect on the cathodic current efficiency of iron ions reduction. Alkalization of the solution leads to a decrease in the proportion of current spent on the reduction of H^+ ions. The formation of poorly soluble REE-oxalates leads to a decrease in the pH of the solution in the range 0.2–0.5, which contributes to the intensification of the process of the cathodic hydrogen evolution.
(3) Increasing of positive charge on the surface of the oxalate precipitate can substitute iron reduction by selective adsorption of REE-oxalates (Makarova et al., 2020a).

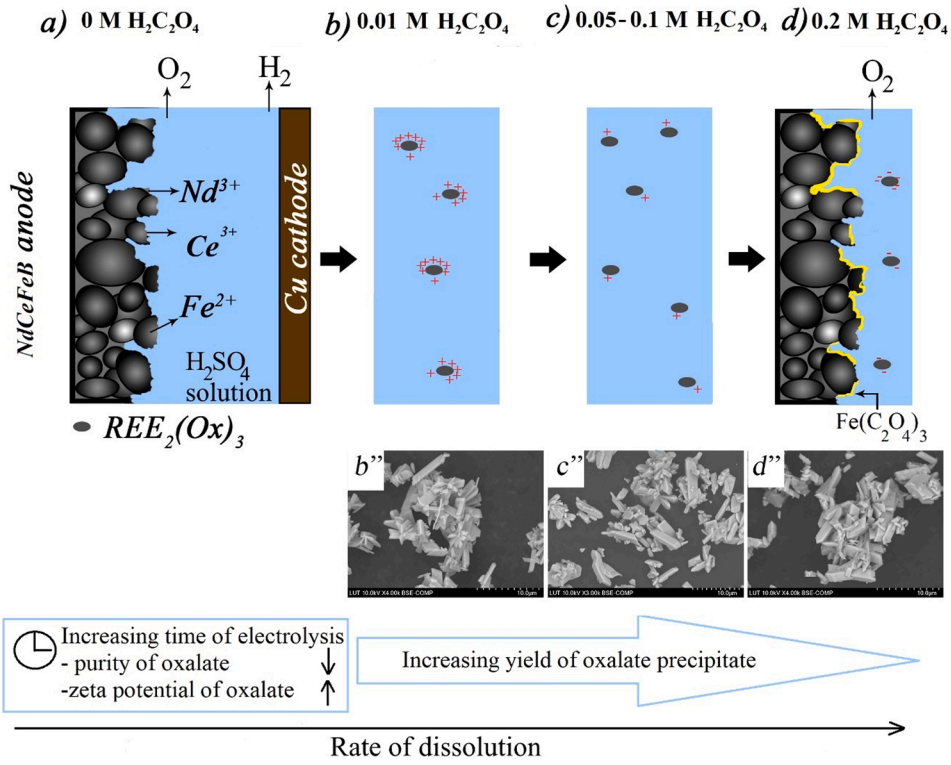

Fig. 8. Proposed mechanism for electrochemical leaching of NdCeFeB magnets in a mixture of 0.5 mol/L H_2SO_4 and $H_2C_2O_4$ (*a* – *d*) and appearance of the precipitated REE-oxalates (*b*" – *d*").

As a summary of the previous Sections, electrochemical dissolution of NdCeFeB magnets can be schematically represented by Fig. 8. The scheme focuses on the influence of $H_2C_2O_4$ concentration on the physico-chemical properties and composition of the REE-oxalates obtained in the process.

The electrochemical dissolution of the NdCeFeB magnet in 0.5 mol/L H_2SO_4 yields a leachate that contains all valuable metals. Addition of oxalic acid during electrolysis allows, on the one side, to intensify the process of the dissolution and, on the other side, to separate rare-earth elements in one step. The purity of the oxalate sediment during electro-leaching varies from 85 to 97% and more than 95% of REEs end up in the precipitate. Increasing the concentration of oxalic acid increases the precipitation yield but also leads to a significant passivation of the magnet surface. On the other hand, low concentration of oxalic acid and long leaching time leads to more positive surface charge of the precipitate and, therefore, to a tendency to attach on the cathode. Depending on the conditions, the REE-oxalates may be recovered as specifically adsorbed precipitate on the cathode or as precipitate formed in the solution.

4. Conclusions

(1) The influence of concentration of oxalic acid that was used in a mixture with sulfuric acid during direct electrochemical leaching of NdCeFeB magnet on properties of rare-earth oxalate precipitate was investigated. Increasing of concentration of oxalic acid has a positive effect on the yield of the REE precipitate but decreases the purity of the oxalate precipitate.

(2) Electro-leaching intensifies the dissolution rate of NdCeFeB magnet by more than 2.5 times when compared with chemical leaching and allows to use higher concentrations of $H_2C_2O_4$ (0.1 and 0.2 M).

(3) Concentration of $H_2C_2O_4$ influences the amount of REE ions both in the solution and in the precipitate. Efficient separation of REEs from other metals in a form of powder in a solution can be achieved at concentrations of $H_2C_2O_4$ from 0.05 to 0.2 mol/L and current density 50 A/dm^2 (yield and purity up to 99.7% and 97.2%, respectively) during electrolysis in 0.5 mol/L sulfuric acid. The finding of this study provides promising data for the scale up experiments. Obtained results will be used in the flow-type electrolyzer that is currently carrying out in our research group.

CRediT authorship contribution statement

Iryna Makarava: Conceptualization, Methodology, Investigation, Formal analysis, Visualization, Writing – original draft. **Aliaksandr Kasach:** Conceptualization, Methodology, Investigation, Formal analysis, Visualization, Writing – original draft. **Dzmitry Kharytonau:** Conceptualization, Writing – review & editing. **Irina Kurilo:** Conceptualization, Writing – review & editing. **Markku Laatikainen:** Conceptualization, Supervision, Methodology, Writing – original draft. **Eveliina Repo:** Project administration, Supervision, Funding acquisition, Methodology, Writing – review & editing.

Declaration of Competing Interest

The authors declare that they have no known competing financial interests or personal relationships that could have appeared to influence the work reported in this paper.

Acknowledgments

The authors thank the European Regional Development Fund 2014−2020 (project code A74334), Maa- ja vesitekniikan tuki ry and Emil Aaltonen Foundation for the financial support. The authors are grateful to Dr. Liisa Puro, Mohammadamin Esmaeli and Andrei Paspelau for their kind support during this project and help in ICP and SEM/EDX measurements.

Appendix A. Supplementary material

Supplementary data to this article can be found online at https://doi.org/10.1016/j.mineng.2022.107446.

References

Abbasalizadeh, A., Seetharaman, S., Venkatesan, P., Sietsma, J., Yang, Y., 2019. Use of iron reactive anode in electrowinning of neodymium from neodymium oxide. Electrochim. Acta 310, 146–152. https://doi.org/10.1016/j.electacta.2019.03.161.

Arsad, A.Z., Ibrahim, N.B., 2016. The effect of Ce doping on the structure, surface morphology and magnetic properties of Dy doped-yttrium iron garnet films prepared by a sol-gel method. J. Magn. Magn. Mater. 410, 128–136. https://doi.org/10.1016/j.jmmm.2016.03.013.

Berzi, L., Dattilo, C.A., Del Pero, F., Delogu, M., Gonzalez, M.I., 2019. Reduced use of rare earth elements for permanent magnet generators: Preliminary results from NEOHIRE project. Procedia Struct. Integr. 24, 961–977. https://doi.org/10.1016/j.prostr.2020.02.084.

Binnemans, K., Jones, P.T., 2014. Perspectives for the recovery of rare earths from end-of-life fluorescent lamps. J. Rare Earths 32 (3), 195–200. https://doi.org/10.1016/S1002-0721(14)60051-X.

Ciacci, L., Vassura, I., Cao, Z., Liu, G., Passarini, F., 2019. Recovering the "new twin": Analysis of secondary neodymium sources and recycling potentials in Europe. Resour. Conserv. Recycl. 142, 143–152. https://doi.org/10.1016/j.resconrec.2018.11.024.

Costis, S., Mueller, K.K., Coudert, L., Neculita, C.M., Reynier, N., Blais, J.-F., 2021. Recovery potential of rare earth elements from mining and industrial residues: A review and cases studies. J. Geochemical Explor. 221, 106699. https://doi.org/10.1016/j.gexplo.2020.106699.

El Wali, M., Golroudbary, S.R., Kraslawski, A., 2021. Circular economy for phosphorus supply chain and its impact on social sustainable development goals. Sci. Total Environ. 777, 146060. https://doi.org/10.1016/j.scitotenv.2021.146060.

Golroudbary, S.R., El Wali, M., Kraslawski, A., 2020. Rationality of using phosphorus primary and secondary sources in circular economy: Game-theory-based analysis. Environ. Sci. Policy 106, 166–176. https://doi.org/10.1016/j.envsci.2020.02.004.

Golroudbary, S.R., Krekhovetckii, N., El Wali, M., Kraslawski, A., 2019. Environmental sustainability of niobium recycling: The case of the automotive industry. Recycling 4, 1–23. https://doi.org/10.3390/recycling4010005.

Jorjani, E., Shahbazi, M., 2016. The production of rare earth elements group via tributyl phosphate extraction and precipitation stripping using oxalic acid. Arab. J. Chem. 9, S1532–S1539. https://doi.org/10.1016/j.arabjc.2012.04.002.

Kumari, A., Sinha, M.K., Pramanik, S., Sahu, S.K., 2018. Recovery of rare earths from spent NdFeB magnets of wind turbine: Leaching and kinetic aspects. Waste Manag. 75, 486–498. https://doi.org/10.1016/j.wasman.2018.01.033.

Lai, W., Liu, M., Li, C., Suo, H., Yue, M., 2014. Recovery of a composite powder from NdFeB slurry by co-precipitation. Hydrometallurgy 150, 27–33. https://doi.org/10.1016/j.hydromet.2014.08.014.

Li, Z.B., Shen, B.G., Zhang, M., Hu, F.X., Sun, J.R., 2015. Substitution of Ce for Nd in preparing $R_2Fe_{14}B$ nanocrystalline magnets. J. Alloys Compd. 628, 325–328. https://doi.org/10.1016/j.jallcom.2014.12.042.

Lin, Q., Lei, C., Zhang, H., Long, X., Xu, J., Liang, F., Wang, R., Zeng, S., He, Y., 2012. Magnetic Studies in Rare Earth-iron Oxalate-bridged Complexes $MFe(C_2O_4)_3{\cdot}9H_2O$ (M=Ce, Pr). Phys. Procedia 25, 369–374. https://doi.org/10.1016/j.phpro.2012.03.098.

Liu, F., Porvali, A., Wang, JinLiang, Wang, H., Peng, C., Wilson, B.P., Lundström, M., 2020. Recovery and separation of rare earths and boron from spent Nd-Fe-B magnets. Miner. Eng. 145, 106097. https://doi.org/10.1016/j.mineng.2019.106097.

Liu, Q., Tu, T., Guo, H., Cheng, H., Wang, X., 2021. High-efficiency simultaneous extraction of rare earth elements and iron from NdFeB waste by oxalic acid leaching. J. Rare Earths 39 (3), 323–330. https://doi.org/10.1016/j.jre.2020.04.020.

Lu, P.-J., Fu, W.-E., Huang, S.-C., Lin, C.-Y., Ho, M.-L., Chen, Y.-P., Cheng, H.-F., 2018. Methodology for sample preparation and size measurement of commercial ZnO nanoparticles. J. Food Drug Anal. 26 (2), 628–636. https://doi.org/10.1016/j.jfda.2017.07.004.

Makarova, I., Dobryden, I., Kharitonov, D., Kasach, A., Ryl, J., Repo, E., Vuorinen, E., 2019. Nickel-nanodiamond coatings electrodeposited from tartrate electrolyte at ambient temperature. Surf. Coatings Technol. 380, 125063. https://doi.org/10.1016/j.surfcoat.2019.125063.

Makarova, I., Ryl, J., Sun, Z., Kurilo, I., Górnicka, K., Laatikainen, M., Repo, E., 2020a. One-step recovery of REE oxalates in electro-leaching of spent NdFeB magnets. Sep. Purif. Technol. 251, 117362. https://doi.org/10.1016/j.seppur.2020.117362.

Makarova, I., Soboleva, E., Osipenko, M., Kurilo, I., Laatikainen, M., Repo, E., 2020b. Electrochemical leaching of rare-earth elements from spent NdFeB magnets. Hydrometallurgy 192, 105264. https://doi.org/10.1016/j.hydromet.2020.105264.

Marins, A.A.L., Banhos, S.G., Muri, E.J.B., Rodrigues, R.V., Cruz, P.C.M., Freitas, M.B.J.G., 2020. Synthesis by coprecipitation with oxalic acid of rare earth and nickel oxides from the anode of spent Ni–MH batteries and its electrochemical properties. Mater. Chem. Phys. 242, 122440. https://doi.org/10.1016/j.matchemphys.2019.122440.

Ni, J., Zhang, Z., Liu, Y., Jia, Z., Huang, B., Yin, Y., 2016. Magnetic properties, microstructure and corrosion behavior of (Pr, Nd)12.6$Fe_{81.3}B_{6.1}$-type sintered magnets doped with (Pr, nd)30Fe62Ga8. Phys. B Condens. Matter 499, 64–69. https://doi.org/10.1016/j.physb.2016.07.008.

Önal, M.A.R., Riaño, S., Binnemans, K., 2020. Alkali baking and solvometallurgical leaching of NdFeB magnets. Hydrometallurgy 191, 105213. https://doi.org/10.1016/j.hydromet.2019.105213.

Ore, I., Pigments, I.O., Rock, P., Crystal, Q., Earths, R., Ash, S., 2021. Mineral commodity summaries.

Peelman, S., Sun, Z.H.I., Sietsma, J., Yang, Y., 2015. Leaching of Rare Earth Elements: Review of Past and Present Technologies. In: Rare Earths Industry. Elsevier, pp. 319–334. https://doi.org/10.1016/B978-0-12-802328-0.00021-8.

Peeters, J.R., Bracqguene, E., Nelen, D., Ueberschaar, M., Van Acker, K., Duflou, J.R., 2018. Forecasting the recycling potential based on waste analysis: A case study for recycling Nd-Fe-B magnets from hard disk drives. J. Clean. Prod. 175, 96–108. https://doi.org/10.1016/j.jclepro.2017.11.080.

Pliego, G., Zazo, J.A., Casas, J.A., Rodriguez, J.J., 2014. Fate of iron oxalates in aqueous solution: The role of temperature, iron species and dissolved oxygen. J. Environ. Chem. Eng. 2 (4), 2236–2241.

Reimer, M.V., Schenk-mathes, H.Y., Hoffmann, M.F., Elwert, T., 2020. Recycling decisions in 2020, 2030, and 2040 — when can substantial NdFeB extraction be expected in the EU analysis of? Metals (Basel). 8, 867. https://doi.org/10.3390/met8110867.

Reisdörfer, G., Bertuol, D., Tanabe, E.H., 2019. Recovery of neodymium from the magnets of hard disk drives using organic acids. Miner. Eng. 143, 105938. https://doi.org/10.1016/j.mineng.2019.105938.

Salmimies, R., Vehmaanperä, P., Häkkinen, A., 2016. Acidic dissolution of magnetite in mixtures of oxalic and sulfuric acid. Hydrometallurgy 163, 91–98. https://doi.org/10.1016/j.hydromet.2016.03.011.

Schreiber, A., Marx, J., Zapp, P., 2019. Comparative life cycle assessment of electricity generation by different wind turbine types. J. Clean. Prod. 233, 561–572. https://doi.org/10.1016/j.jclepro.2019.06.058.

Tian, Y., Liu, Z., Zhang, G., 2019. Recovering REEs from NdFeB wastes with high purity and efficiency by leaching and selective precipitation process with modified agents. J. Rare Earths 37 (2), 205–210. https://doi.org/10.1016/j.jre.2018.10.002.

Turpeinen, E., Saavalainen, P., Oravisj, K., Omodara, L., Pitk, S., Keiski, R.L., 2019. Recycling and substitution of light rare earth elements, cerium, lanthanum, neodymium, and praseodymium from end-of-life applications - A review. J. Clean. Prod. 236, 117573. https://doi.org/10.1016/j.jclepro.2019.07.048.

Venkatesan, P., Sun, Z.H.I., Sietsma, J., Yang, Y., 2018. An environmentally friendly electro-oxidative approach to recover valuable elements from NdFeB magnet waste. Sep. Purif. Technol. 191, 384–391. https://doi.org/10.1016/j.seppur.2017.09.053.

Xu, J., Axinte, E., Zhao, Z., Wang, Y., 2016. Effect of C and Ce addition on the microstructure and magnetic property of the mechanically alloyed FeSiBAlNi high entropy alloys. J. Magn. Magn. Mater. 414, 59–68. https://doi.org/10.1016/j.jmmm.2016.04.067.

Yang, L., Bi, M., Jiang, J., Ding, X., Zhu, M., Li, W., Lv, Z., Song, Z., 2017a. Effect of cerium on the corrosion behaviour of sintered (Nd, Ce)FeB magnet. J. Magn. Magn. Mater. 432, 181–189. https://doi.org/10.1016/j.jmmm.2017.01.094.

Yang, Y., Lan, C., Wang, Y., Zhao, Z., Li, B., 2020. Recycling of ultrafine NdFeB waste by the selective precipitation of rare earth and the electrodeposition of iron in hydrofluoric acid. Sep. Purif. Technol. 230, 115870. https://doi.org/10.1016/j.seppur.2019.115870.

Yang, Y., Walton, A., Sheridan, R., Güth, K., Gauß, R., Gutfleisch, O., Buchert, M., Steenari, B.-M., Van Gerven, T., Jones, P.T., Binnemans, K., 2017b. REE Recovery from End-of-Life NdFeB Permanent Magnet Scrap: A Critical Review. J. Sustain. Metall. 3 (1), 122–149. https://doi.org/10.1007/s40831-016-0090-4.

Zhang, W., Noble, A., Ji, B., Li, Q., 2020. Effects of contaminant metal ions on precipitation recovery of rare earth elements using oxalic acid. J. Rare Earths. https://doi.org/10.1016/j.jre.2020.11.008.